

First Principle Study for Optical Properties of TMDC/Graphene Heterostructures

Cheng-Hsien Yang (楊承憲)* and Shu-Tong Chang

Department of Electrical Engineering, National Chung Hsing University, Taichung 40227, Taiwan

The transition-metal dichalcogenide (TMDC) in the family of MX_2 ($\text{M} = \text{Mo, W}; \text{X} = \text{S, Se}$) and the graphene (Gr) monolayer are an atomically thin semiconductor and a semimetal, respectively. The monolayer MX_2 has been discovered as a new class of semiconductors for electronics and optoelectronics applications. Because of the hexagonal lattice structure of both materials, MX_2 and Gr are often combined with each other to generate van der Waals heterostructures. Here, the MX_2/Gr heterostructures are investigated theoretically based on density functional theory (DFT). The electronic structure and the optical properties of four different MX_2/Gr heterostructures are computed. We systematically compare these MX_2/Gr heterostructures for their complex permittivity, absorption coefficient, reflectivity and refractive index.

I. INTRODUCTION

Materials in confined geometries are hosts to novel phenomena. For example, in one dimension (1D), the fractional charge excitation or the soliton is found in the electronic properties of the organic polyacetylene [1], and the Haldane conjecture [2], which corresponds to the symmetry-protected topological phase, is experimentally found in the spin-1 magnetic chain, e.g., CsNiCl_3 , $[\text{Ni}(\text{HF}_2)(3\text{-C}l\text{pyradine})_4]\text{BF}_4$, $\text{Ni}(\text{C}_2\text{H}_8\text{N}_2)_2\text{NO}_2(\text{ClO}_4)$ and Y_2BaNiO_5 [3–8]. Quantum states conversion through entanglement manipulations [9] as well as new types of quantum phase transitions with a negative central charge [10] are among the recently investigated 1D systems.

Examples of novel physical phenomena in two dimension (2D) include quantum Hall systems in semiconductors [11], the supersolid phase of atomic systems in the optical lattice [12, 13] and Dirac electrons in graphene [14]. Graphene (Gr) is one of the most widely investigated 2D materials; it possesses a high mobility [15–19] and is driven by Dirac cone dispersions near the Fermi level at the K-point and the K'-point in the hexagonal Brillouin zone[20]. However, the gapless nature of Gr limits its applications in the semiconductor industry. Therefore, finding new 2D materials with a large band gap is an interesting topic. Note that a new allotropy of carbon, the 2D biphenylene monolayer, was discovered very recently [21–24].

In addition to the carbon, a number of 2D materials with an energy band gap have been synthesized, including the quantum spin Hall insulator HgTe [25, 26], free-standing silicene [27] and the transition-metal dichalcogenide (TMDC) family. Monolayer TMDCs [28–39], such as molybdenum disulfide (MoS_2) [40, 41], molybdenum diselenide (MoSe_2) [42], tungsten disulfide (WS_2) [43] and tungsten diselenide (WSe_2) [44, 45], have been found to be direct gap semiconductors [46] and have emerged as new optically active materials for novel device applications. The TMDCs in the family of MX_2 , where

$\text{M} = \text{Mo, W}$ and $\text{X} = \text{S, Se}$, have a rather large energy band gap compared to HgTe and silicene; thus, these materials are more versatile as candidates for thin, flexible device applications and useful for a variety of applications including transistors [47], lubrication [48], lithium-ion batteries [49] and thermoelectric devices [50]. Other TMDCs, e.g., PbTaSe_2 , $\text{Mo}_x\text{W}_{1-x}\text{Te}_2$ and NiTe_2 , can exhibit more unusual physical properties such as topological superconductivity and Dirac and Weyl semimetal physics [51–56]. Two-dimensional hydrogenated NiTe_2 , PdS_2 , PdSe_2 , and PtSe_2 monolayers also exhibit a quantum anomalous Hall effect [57].

One of the approaches used to broaden the application of 2D materials is to form a heterostructure in which similar lattice structures for different monolayers are usually required, e.g., the hexagonal lattices of TMDC, Gr, boron nitride [58], and boron phosphide (BP) [59]. It has been suggested that MX_2/BP heterostructures have a good ability for optical absorption [59]. On the other hand, the MX_2/Gr of the type-I van der Waals heterostructures have attracted much attention for their electronic properties. Research on MoS_2/Gr [60–62], MoSe_2/Gr [63–65], WS_2/Gr [66] and WSe_2/Gr [67, 68] has revealed that MX_2/Gr is favorable for electronics applications and field-effect transistors. However, there are relatively few studies on its optical properties [69–71]; therefore, comprehensive research on the optical properties of MX_2/Gr is desired.

In this communication, we theoretically investigate the optical properties of MX_2/Gr heterostructures. By means of a density functional theory simulation, we systematically compare the energy band structures, the density of states, complex permittivity, absorption coefficients, reflectivity, and refraction indexes.

II. MATERIALS AND METHODS

The first-principles calculations are based on the local-density approximation (LDA) proposed by Kohn and Sham [72], which approximates the total energy of the multielectron system. The simulations were implemented using the software package NANODCAL and its accom-

* d104064006@mail.nchu.edu.tw

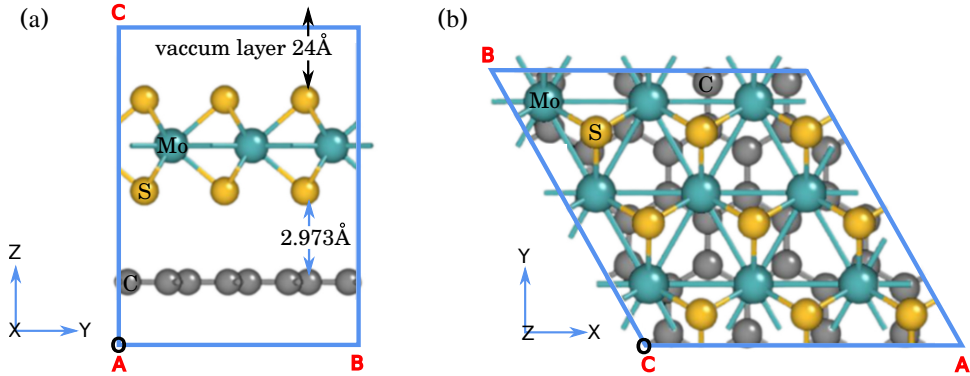


FIG. 1. The stacking of the 3×3 MoS₂ supercell and the 4×4 Gr supercell. (a) The side view. (b) The top view. For the other MX₂/Gr, the atom–atom distances are listed in Table II.

panying software packages DEVICESTUDIO and OPTICAL [73, 74]. A plane wave basis was set with a cutoff energy of 80 Hartree and a $5 \times 5 \times 1$ Γ -centered k -points grid. The atomic structures were relaxed until the force was smaller than 0.03 eV/Å and the total energy convergence criterion was set as 10^{-4} eV. In order to avoid interactions in the vertical direction between neighboring slabs, a vacuum layer of 24 Å was added between different slabs.

The lattice constants of the MoS₂, MoSe₂, WS₂, WSe₂ and Gr monolayers were 3.166 Å, 3.288 Å, 3.153 Å, 3.282 Å and 2.47 Å, respectively[32, 63]. For all the MX₂/Gr heterostructures, lattice mismatch ratios less than 5% were achieved by choosing a 3×3 MX₂ supercell and a 4×4 Gr supercell, as shown in Figure 1. The details of the lattice mismatch ratios are listed in Table I. After the structure optimization, the lattice contents were 9.668 Å, 9.854 Å, 9.648 Å and 9.845 Å for MoS₂/Gr, MoSe₂/Gr, WS₂/Gr and WSe₂/Gr, respectively. The details of the atom–atom distances as well as the MX₂ layer–Gr layer distances are listed in Table II. The total number of atoms in the simulations was 59 for MX₂/Gr, 27 for the 3×3 monolayer of MX₂, and 32 for the 4×4 monolayer of Gr.

The binding energies E_b are calculated by the energy difference between the heterostructures and the monolayers:

$$E_b = E_{\text{MX}_2/\text{Gr}} - E_{\text{MX}_2} - E_{\text{Gr}}, \quad (1)$$

where $E_{\text{MX}_2/\text{Gr}}$, E_{MX_2} and E_{Gr} are the total energies of the heterostructures, isolated MX₂ and Gr, respectively. It is interesting to compare other heterostructures,

TABLE I. The lattice mismatch ratios and the biding energies of TMDCs/graphene with 3×3 supercell of MX₂ and 4×4 supercell of graphene.

MX ₂ /Gr	MoS ₂ /Gr	MoSe ₂ /Gr	WS ₂ /Gr	WSe ₂ /Gr
mismatch ratio	1.83%	0.10%	2.04%	0.01%
E_b	-194 meV	-146 meV	-178 meV	-246 meV

such as MX₂/BP [59], as regards binding energies. The interface binding energies of the most stable configurations of MoS₂/BP, MoSe₂/BP, WS₂/BP and WSe₂/BP are -196 meV, -130 meV, -201 meV and -141 meV, respectively, [59]. As listed in Table I, all the binding energies for the MX₂/Gr heterostructures in this study are negative, and the values are close to MX₂/BP, demonstrating that the structural stability of MX₂/Gr is similar to that of MX₂/BP.

III. RESULTS

A. Band structures

The direct band gaps of the MoS₂, MoSe₂, WS₂ and WSe₂ monolayers were 1.82 eV, 1.56 eV, 1.95 eV and 1.64 eV, respectively, [36], where both the conduction band minimum (CBM) and the valence band maximum (VBM) were at the K-point in the Brillouin zone. The Dirac point of the Gr was located at the K-point and pinned to the Fermi level. All the results of the energy band structures for the MX₂ monolayers are consistent with the existing literature [17, 35]. Now we report the energy band structures and the electronic density of states (DOS) for the four MX₂/Gr, as shown in Figure 2. We found that the band structure of MX₂/Gr could basically be regarded as the overlap of the band struc-

TABLE II. The optimized atom–atom distances as well as the MX₂ layer – Gr layer distances.

MoS ₂ /Gr	Mo-S	Mo-C	S-C	C-C	MoS ₂ -Gr
	2.404 Å	4.826 Å	3.089 Å	1.600 Å	2.973 Å
MoSe ₂ /Gr	Mo-Se	Mo-C	Se-C	C-C	MoSe ₂ -Gr
	2.349 Å	4.920 Å	3.270 Å	1.626 Å	3.161 Å
WS ₂ /Gr	W-S	W-C	S-C	C-C	WS ₂ -Gr
	2.379 Å	4.774 Å	3.078 Å	1.596 Å	2.954 Å
WSe ₂ /Gr	W-Se	W-C	Se-C	C-C	WSe ₂ -Gr
	2.354 Å	4.940 Å	3.286 Å	1.625 Å	3.178 Å

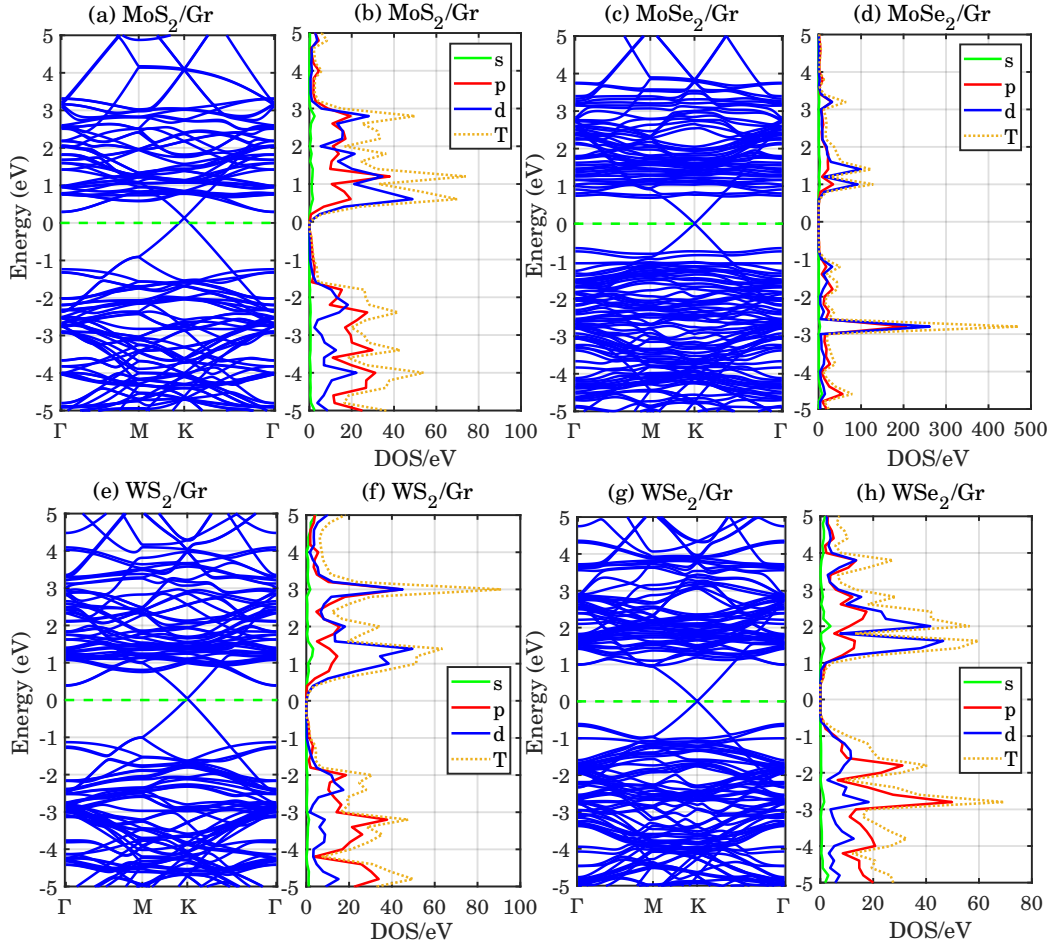


FIG. 2. The energy band structures and the DOS for the MX_2/Gr van der Waals heterostructures. The partial DOS values are labeled with s, p, or d, corresponding to the orbital contributions, and the total DOS is labeled with T. (a,b) MoS_2/Gr , (c,d) MoSe_2/Gr , (e,f) WS_2/Gr , (g,h) WSe_2/Gr .

tures of the MX_2 and Gr monolayers. Due to van der Waals interactions, the Dirac point opens a small gap of 8.3 meV, 7.9 meV, 8.86 meV and 3.53 meV for MoS_2/Gr , MoSe_2/Gr , WS_2/Gr and WSe_2/Gr , respectively. The total and partial DOS values of MX_2/Gr are also shown in Figure 2. The partial DOS is the relative contribution of a particular orbital to the total DOS. The d-orbital contributions mainly come from the W or Mo atoms, and the p-orbital contributions come from S or Se, and C atoms. Contributions from the s-orbital are minimal. These results reflect a fairly weak interfacial coupling at the interface between MX_2 and Gr.

The Schottky contacts are formed between the semiconducting MX_2 and the metallic Gr. The Schottky barrier is one of the most important characteristics of a semiconductor–metal junction and dominates the transport properties. Based on the Schottky–Mott model [75–77], at the interface of the metal and semiconductor, an n-type Schottky barrier height (SBH) Φ_{Bn} is defined as the energy difference between the Fermi level E_F and the conduction band minimum E_C , i.e., $\Phi_{Bn} = E_C - E_F$. Similarly, the p-type SBH Φ_{Bp} is defined as the energy

difference between E_F and the valence band maximum E_V , i.e., $\Phi_{Bp} = E_F - E_V$. The n/p-type Schottky contacts are classified by the smaller SBH. The SBH are $\Phi_{Bn} = 0.29$ eV and $\Phi_{Bp} = 1.23$ eV for MoS_2/Gr , $\Phi_{Bn} = 0.75$ eV and $\Phi_{Bp} = 0.65$ eV for MoSe_2/Gr , $\Phi_{Bn} = 0.39$ eV and $\Phi_{Bp} = 1.13$ eV for WS_2/Gr , and $\Phi_{Bn} = 1.00$ eV and $\Phi_{Bp} = 0.61$ eV for WSe_2/Gr , respectively. Therefore, MoS_2/Gr , MoSe_2/Gr , WS_2/Gr and WSe_2/Gr are the n-type, p-type, n-type and p-type Schottky contacts, respectively[64, 66, 67].

B. Optical properties

In order to understand the optical properties, the complex permittivity or the so-called dielectric function was computed under the long-wave approximation, i.e., $\vec{q} = 0$. The complex permittivity $\varepsilon(\omega) = \varepsilon_{\text{real}}(\omega) + \varepsilon_{\text{imag}}(\omega)$ as

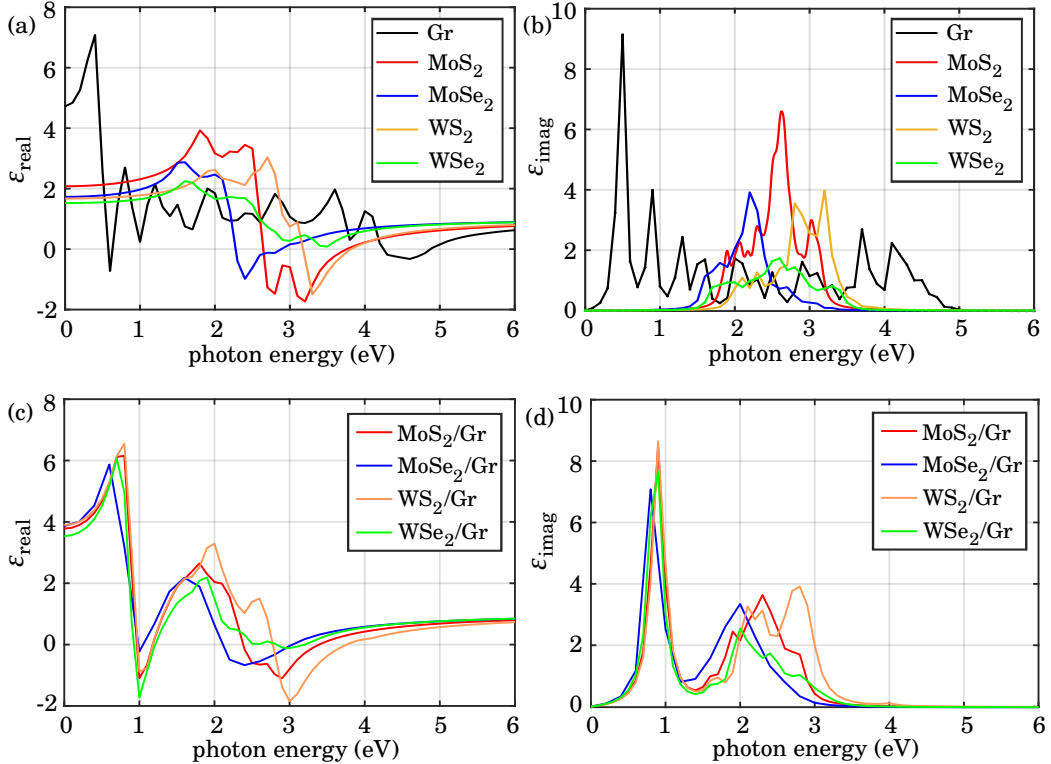


FIG. 3. The complex permittivities for MX₂/Gr heterostructures and MX₂ and Gr monolayers as functions of incident photon energy. (a),(c) The real part of the permittivity ε_{real}. (b),(d) The imaginary part of the permittivity ε_{imag}.

a function of incident photon energy is [78]

$$\varepsilon(\omega) = 1 + \frac{2e^2}{\varepsilon_0 m^2} \frac{1}{V} \sum_{\alpha\beta} \frac{|\langle \psi_\beta | \hat{e} \cdot \vec{p} | \psi_\alpha \rangle|^2}{(E_\beta - E_\alpha)^2 / \hbar^2} \frac{f(E_\alpha) - f(E_\beta)}{E_\beta - E_\alpha - \hbar\omega - i\kappa} \quad (2)$$

where e is the electron charge, ε_0 is the vacuum permittivity, m is the electron mass, \hat{e} is the direction of the vector potential, \vec{p} is the momentum operator, $\hbar\omega$ is the photon energy, and $f(E_\alpha)$ and $f(E_\beta)$ are the Fermi-Dirac distribution functions. Since $\varepsilon = n_c^2$, i.e., $\varepsilon_{\text{real}} + i\varepsilon_{\text{imag}} = (n + i\kappa)^2$, the refraction index n and the extinction coefficient κ are obtained:

$$n^2 = \frac{|\varepsilon| + \varepsilon_{\text{real}}}{2}, \quad (3)$$

$$\kappa^2 = \frac{|\varepsilon| - \varepsilon_{\text{real}}}{2}. \quad (4)$$

The real part ε_{real} is caused by various kinds of displacement polarization inside the material and represents the energy storage term of the material. The imaginary part ε_{imag} is related to the absorption of the material, including gain and loss. Therefore, the permittivity must be real in the absence of the incident photon energy, i.e., $\varepsilon(\omega = 0) = \varepsilon_{\text{real}}$. It is expected that the smaller the energy gap of a material, the larger its ε(0). On the other hand, since the DOS only appears in a finite range of energy in the numerical simulation, electron transitions

by the absorption of photons do not occur if the photon energy is too large. Therefore, without photon absorption the computed ε_{imag} is close to zero in the large limit of the incident photon energy, and the permittivity approaches a constant real value.

In Figure 3, we show the real part and the imaginary part of the complex permittivity for MX₂/Gr heterostructures and MX₂ and Gr monolayers. Since the energies corresponding to the peak positions of the DOS in the conduction and valence bands of the MX₂/Gr were smaller than those of MX₂, the peak positions of the real part ε_{real}(ω) of MX₂/Gr in Fig. 3(c) had a red shift compared with the MX₂ in Fig. 3(a). The highest peak corresponding energy of the imaginary part ε_{imag}(ω) of the MX₂/Gr in Fig. 3(d) was about 0.8 eV to 0.9 eV, which corresponds to the position where the real part decreases the fastest.

After obtaining the dielectric function, the absorption coefficient α is computed by

$$\alpha = \frac{2\omega\kappa}{c}, \quad (5)$$

and the reflectivity R is

$$R = \frac{(n - 1)^2 + \kappa^2}{(n + 1)^2 + \kappa^2}. \quad (6)$$

Figure 4 compares MX₂/Gr, MX₂ and Gr for their absorption coefficient α, reflectivity R and refractive index n . Since MX₂/Gr has a smaller optical band gap

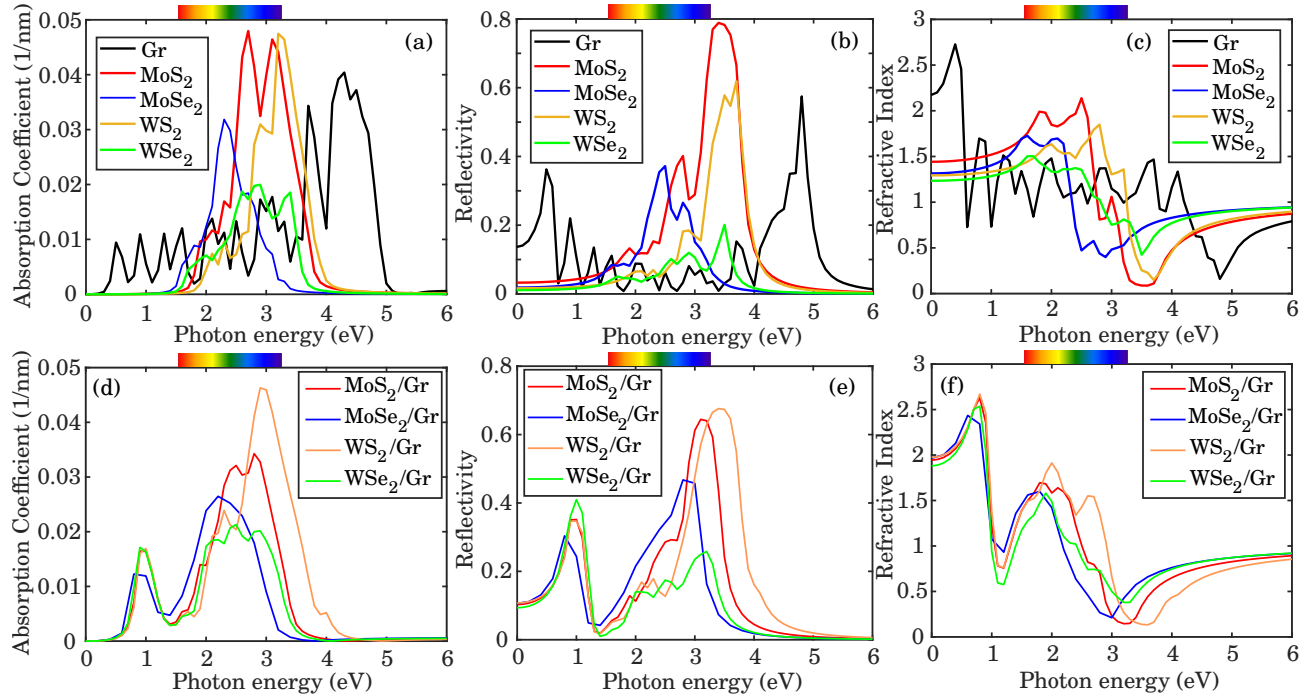


FIG. 4. The comparison of MX_2/Gr heterostructures and MX_2 and Gr monolayers according to their (a),(d) absorption coefficient α , (b),(e) reflectivity R and (c),(f) refractive index n . The rainbow bars represent the energy range of visible light, from 1.59 eV to 3.26 eV.

compared with the MX_2 monolayer, MX_2/Gr has a wider range of light absorption, from 0.6 eV to 4 eV. As shown in Fig. 4(b),(e), MX_2/Gr had a higher reflectivity than MX_2 in the infrared area ($\hbar\omega < 1.2$ eV), and had a higher reflectivity than Gr in the visible light area. We compare the real part of the permittivity of monolayer MX_2 in Fig. 3(a) with the refractive index of monolayer MX_2 in Fig. 4(c), and compare the real part of the permittivity of the MX_2/Gr heterostructure in Fig. 3(c) with that of MX_2/Gr in Fig. 4(f). It was found that the changing trends from Fig. 3(a) to Fig. 4(c) are similar to those from Fig. 3(c) to Fig. 4(f). This means that the real part of the dielectric constant dominates the effect of the refractive index. The above simulation results suggest that MX_2/Gr heterostructures are good candidate materials for optical applications.

IV. DISCUSSION

Two-dimensional heterostructures based on TMDCs exhibit the enhancement of electrical and optoelectrical properties, which are promising for next-generation optoelectronics devices. We systematically computed the complex permittivity $\varepsilon(\omega)$, absorption coefficient $\alpha(\omega)$, reflectivity $R(\omega)$ and refractive index $n(\omega)$ for MX_2/Gr heterostructures, where M = Mo, W; and X = S, Se. Our

results qualitatively agree with those from previous studies on MoS_2/Gr [69] and WSe_2/Gr [70], where red shifts in the $\alpha(\omega)$, $R(\omega)$ and $n(\omega)$ were found compared with MoS_2 and WSe_2 monolayers. We extended the investigations to other MX_2/Gr heterostructures, and found qualitatively similar behavior in their optical properties.

It is worth comparing our MX_2/Gr results with the recent simulation results on the MX_2/BP in terms of absorption abilities [59]. Although different types of van der Waals heterostructures were found in MX_2/BP (type-I for MoS_2/BP and WS_2/BP ; type-II for MoSe_2/BP and WSe_2/BP), all the materials of MX_2/BP have excellent absorption abilities in the infrared and visible light range, i.e., $\alpha(\omega) \approx 0.01 \text{ nm}^{-1}$ to 0.05 nm^{-1} for the wavelength $400 \text{ nm} \leq \lambda \leq 1200 \text{ nm}$ [59]. In our study, all the MX_2/Gr were type-I heterostructures, and the values of the absorption coefficients were in the same range compared with MX_2/BP in the infrared and visible light range. Therefore, MX_2/Gr can be utilized as alternative materials for the applications of solar optoelectronics devices.

ACKNOWLEDGMENTS

CHY is grateful to Dr. Yu-Chin Tzeng for his invaluable discussions and helps.

- [1] W. P. Su, J. R. Schrieffer, and A. J. Heeger, *Phys. Rev. Lett.* **42**, 1698 (1979).
- [2] F. D. M. Haldane, *Phys. Rev. Lett.* **50**, 1153 (1983).
- [3] G. Xu, J. F. DiTusa, T. Ito, K. Oka, H. Takagi, C. Broholm, and G. Aeppli, *Phys. Rev. B* **54**, R6827 (1996).
- [4] W. J. L. Buyers, R. M. Morra, R. L. Armstrong, M. J. Hogan, P. Gerlach, and K. Hirakawa, *Phys. Rev. Lett.* **56**, 371 (1986).
- [5] J. P. Renard, M. Verdaguer, L. P. Regnault, W. A. C. Erkelens, J. Rossat-Mignod, and W. G. Stirling, *Europhysics Letters* **3**, 945 (1987).
- [6] Y.-C. Tzeng, *Phys. Rev. B* **86**, 024403 (2012).
- [7] Y.-C. Tzeng, H. Onishi, T. Okubo, and Y.-J. Kao, *Phys. Rev. B* **96**, 060404 (2017).
- [8] D. M. Pajerowski, A. P. Podlesnyak, J. Herbrych, and J. Manson, *Phys. Rev. B* **105**, 134420 (2022).
- [9] Y.-C. Tzeng, L. Dai, M. Chung, L. Amico, and L.-C. Kwek, *Sci. Rep.* **6**, 26453 (2016).
- [10] Y.-T. Tu, Y.-C. Tzeng, and P.-Y. Chang, *SciPost Phys.* **12**, 194 (2022).
- [11] K. v. Klitzing, G. Dorda, and M. Pepper, *Phys. Rev. Lett.* **45**, 494 (1980).
- [12] K.-K. Ng, Y.-C. Chen, and Y.-C. Tzeng, *J. Phys.: Cond. Mat.* **22**, 185601 (2010).
- [13] Y.-C. Chen and M.-F. Yang, *Journal of Physics Communications* **1**, 035009 (2017).
- [14] A. K. Geim, *Science* **324**, 1530 (2009).
- [15] K. I. Bolotin, K. J. Sikes, Z. Jiang, M. Klima, G. Fudenberg, J. Hone, P. Kim, and H. L. Stormer, *Solid State Communications* **146**, 351 (2008).
- [16] K. T. Chan, J. B. Neaton, and M. L. Cohen, *Phys. Rev. B* **77**, 235430 (2008).
- [17] Z. Torbatian and R. Asgari, *Applied Sciences* **8**, 238 (2018).
- [18] E. N. Koukaras, G. Kalosakas, C. Gallois, and K. Papagelis, *Sci. Rep.* **5**, 12923 (2015).
- [19] F. Wendler, A. Knorr, and E. Malic, *Nanophotonics* **4**, 224 (2015).
- [20] A. H. Castro Neto, F. Guinea, N. M. R. Peres, K. S. Novoselov, and A. K. Geim, *Rev. Mod. Phys.* **81**, 109 (2009).
- [21] Q. Fan, L. Yan, M. W. Tripp, *et al.*, *Science* **372**, 852 (2021).
- [22] H. K. Al-Jayyousi, M. Sajjad, K. Liao, and N. Singh, *Sci. Rep.* **12**, 4653 (2022).
- [23] A. Bafeekry, M. Faraji, M. M. Fadlallah, H. R. Jappor, S. Karbasizadeh, M. Ghergherehchi, and D. Gogova, *J. Phys.: Cond. Mat.* **34**, 015001 (2021).
- [24] K. Ren, H. Shu, W. Huo, Z. Cui, and Y. Xu, *Nanotechnology* **33**, 345701 (2022).
- [25] B. A. Bernevig, T. L. Hughes, and S.-C. Zhang, *Science* **314**, 1757 (2006).
- [26] M. König, S. Wiedmann, C. Brüne, A. Roth, H. Buhmann, L. W. Molenkamp, X.-L. Qi, and S.-C. Zhang, *Science* **318**, 766 (2007).
- [27] P. Vogt, P. De Padova, C. Quaresima, J. Avila, E. Frantzeskakis, M. C. Asensio, A. Resta, B. Ealet, and G. Le Lay, *Phys. Rev. Lett.* **108**, 155501 (2012).
- [28] J. N. Coleman, M. Lotya, A. O'Neill, S. D. Bergin, P. J. King, U. Khan, K. Young, A. Gaucher, S. De, R. J. Smith, I. V. Shvets, S. K. Arora, G. Stanton, H.-Y. Kim, K. Lee, G. T. Kim, G. S. Duesberg, T. Hallam, J. J. Boland, J. J. Wang, J. F. Donegan, J. C. Grunlan, G. Moriarty, A. Shmeliov, R. J. Nicholls, J. M. Perkins, E. M. Grieveson, K. Theuwissen, D. W. McComb, P. D. Nellist, and V. Nicolosi, *Science* **331**, 568 (2011).
- [29] D. W. Lutzke, W. Zhang, A. Suslu, T.-R. Chang, H. Lin, H.-T. Jeng, S. Tongay, J. Wu, A. Bansil, and A. Lanzara, *Phys. Rev. B* **91**, 235202 (2015).
- [30] W.-T. Hsu, L.-S. Lu, D. Wang, J.-K. Huang, M.-Y. Li, T.-R. Chang, Y.-C. Chou, Z.-Y. Juang, H.-T. Jeng, L.-J. Li, *et al.*, *Nature Communications* **8**, 1 (2017).
- [31] Y. Zhang, T.-R. Chang, B. Zhou, Y.-T. Cui, H. Yan, Z. Liu, F. Schmitt, J. Lee, R. Moore, Y. Chen, H. Lin, H.-T. Jeng, S.-K. Mo, Z. Hussain, A. Bansil, and Z.-X. Shen, *Nature Nanotechnology* **9**, 111 (2014).
- [32] C.-H. Yang, Y.-F. Chung, Y.-S. Su, K.-T. Chen, Y.-S. Huang, and S.-T. Chang, *J. Comput. Electron.* **21**, 571 (2022).
- [33] S. Kumar and U. Schwingenschlogl, *Chemistry of Materials* **27**, 1278 (2015).
- [34] A. Kormányos, G. Burkard, M. Gmitra, J. Fabian, V. Zólyomi, N. D. Drummond, and V. Fal'ko, *2D Materials* **2**, 022001 (2015).
- [35] T. Cheiwchanwathanig and W. R. L. Lambrecht, *Phys. Rev. B* **85**, 205302 (2012).
- [36] S. Haldar, H. Vovusha, M. K. Yadav, O. Eriksson, and B. Sanyal, *Phys. Rev. B* **92**, 235408 (2015).
- [37] J. Gusakova, X. Wang, L. L. Shiau, A. Krivosheeva, V. Shaposhnikov, V. Borisenko, V. Gusakov, and B. K. Tay, *Physica Status Solidi A* **214**, 1700218 (2017).
- [38] A. Molina-Sánchez and L. Wirtz, *Phys. Rev. B* **84**, 155413 (2011).
- [39] X. Gu and R. Yang, *Applied Physics Letters* **105**, 131903 (2014).
- [40] T.-R. Chang, H. Lin, H.-T. Jeng, and A. Bansil, *Sci. Rep.* **4**, 6270 (2014).
- [41] A. Splendiani, L. Sun, Y. Zhang, T. Li, J. Kim, C.-Y. Chim, G. Galli, and F. Wang, *Nano letters* **10**, 1271 (2010).
- [42] S. Helmrich, K. Sampson, D. Huang, M. Selig, K. Hao, K. Tran, A. Achstein, C. Young, A. Knorr, E. Malic, U. Woggon, N. Owschimikow, and X. Li, *Phys. Rev. Lett.* **127**, 157403 (2021).
- [43] H. R. Gutiérrez, N. Perea-López, A. L. Elías, A. Berkdemir, B. Wang, R. Lv, F. López-Urías, V. H. Crespi, H. Terrones, and M. Terrones, *Nano Letters* **13**, 3447 (2013).
- [44] H. Zhou, C. Wang, J. C. Shaw, R. Cheng, Y. Chen, X. Huang, Y. Liu, N. O. Weiss, Z. Lin, Y. Huang, and X. Duan, *Nano Letters* **15**, 709 (2015).
- [45] R.-Y. Liu, M.-K. Lin, P. Chen, T. Suzuki, P. C. J. Clark, N. K. Lewis, C. Cacho, E. Springate, C.-S. Chang, K. Okazaki, W. Flavell, I. Matsuda, and T.-C. Chiang, *Phys. Rev. B* **100**, 214309 (2019).
- [46] K. F. Mak, C. Lee, J. Hone, J. Shan, and T. F. Heinz, *Phys. Rev. Lett.* **105**, 136805 (2010).
- [47] Y. Yoon, K. Ganapathi, and S. Salahuddin, *Nano Letters* **11**, 3768 (2011).
- [48] C. Lee, Q. Li, W. Kalb, X.-Z. Liu, H. Berger, R. W. Carpick, and J. Hone, *Science* **328**, 76 (2010).
- [49] K. Chang and W. Chen, *Chem. Commun.* **47**, 4252

- (2011).
- [50] M. R. Jobayr and E. M.-T. Salman, *Chin. J. Phys.* **74**, 270 (2021).
- [51] T.-R. Chang, P.-J. Chen, G. Bian, S.-M. Huang, H. Zheng, T. Neupert, R. Sankar, S.-Y. Xu, I. Belopolski, G. Chang, B. Wang, F. Chou, A. Bansil, H.-T. Jeng, H. Lin, and M. Z. Hasan, *Phys. Rev. B* **93**, 245130 (2016).
- [52] G. Bian, T.-R. Chang, R. Sankar, S.-Y. Xu, H. Zheng, T. Neupert, C.-K. Chiu, S.-M. Huang, G. Chang, I. Belopolski, D. S. Sanchez, M. Neupane, N. Alidoust, C. Liu, B. Wang, C.-C. Lee, H.-T. Jeng, C. Zhang, Z. Yuan, S. Jia, A. Bansil, F. Chou, H. Lin, and M. Z. Hasan, *Nature Communications* **7**, 1 (2016).
- [53] T.-R. Chang, S.-Y. Xu, G. Chang, C.-C. Lee, S.-M. Huang, B. Wang, G. Bian, H. Zheng, D. S. Sanchez, I. Belopolski, N. Alidoust, M. Neupane, A. Bansil, H.-T. Jeng, H. Lin, and M. Z. Hasan, *Nature communications* **7**, 1 (2016).
- [54] Y.-C. Tzeng and M.-F. Yang, *Phys. Rev. B* **102**, 035148 (2020).
- [55] A. Sufyan, G. Macam, C.-H. Hsu, Z.-Q. Huang, S.-M. Huang, H. Lin, and F.-C. Chuang, *Chin. J. Phys.* **73**, 95 (2021).
- [56] J. A. Hlevyack, L.-Y. Feng, M.-K. Lin, R. A. B. Villaos, R.-Y. Liu, P. Chen, Y. Li, S.-K. Mo, F.-C. Chuang, and T.-C. Chiang, *npj 2D Materials and Applications* **5**, 1 (2021).
- [57] L.-Y. Feng, R. A. B. Villaos, H. N. Cruzado, Z.-Q. Huang, C.-H. Hsu, H.-C. Hsueh, H. Lin, and F.-C. Chuang, *Chin. J. Phys.* **66**, 15 (2020).
- [58] C. Yelgel, Ö. C. Yelgel, and O. Gülsären, *Journal of Applied Physics* **122**, 065303 (2017).
- [59] K. Ren, M. Sun, Y. Luo, S. Wang, J. Yu, and W. Tang, *Applied Surface Science* **476**, 70 (2019).
- [60] H. V. Phuc, N. N. Hieu, B. D. Hoi, L. T. T. Phuong, and C. V. Nguyen, *Surface Science* **668**, 23 (2018).
- [61] C. V. Nguyen, *Superlattices and Microstructures* **116**, 79 (2018).
- [62] Y. Ma, Y. Dai, M. Guo, C. Niu, and B. Huang, *Nanoscale* **3**, 3883 (2011).
- [63] Y. Ma, Y. Dai, W. Wei, C. Niu, L. Yu, and B. Huang, *J. Phys. Chem. C* **115**, 20237 (2011).
- [64] W. Zhang, G. Hao, R. Zhang, J. Xu, X. Ye, and H. Li, *Journal of Physics and Chemistry of Solids* **157**, 110189 (2021).
- [65] G.-Q. Hao, R. Zhang, W.-J. Zhang, N. Chen, X.-J. Ye, and H.-B. Li, *Acta Physica Sinica* **71**, 017104 (2022).
- [66] J. Zheng, E. Li, D. Ma, Z. Cui, T. Peng, and X. Wang, *Physica Status Solidi B* **256**, 1900161 (2019).
- [67] X. Zhang, Y. Sun, W. Gao, Y. Lin, X. Zhao, Q. Wang, X. Yao, M. He, X. Ye, and Y. Liu, *RSC advances* **9**, 18157 (2019).
- [68] H.-H. Ma, X.-B. Zhang, X.-Y. Wei, and J.-M. Cao, *Acta Physica Sinica* **69**, 117101 (2020).
- [69] B. Qiu, X. Zhao, G. Hu, W. Yue, J. Ren, and X. Yuan, *Nanomaterials* **8**, 962 (2018).
- [70] B. Qiu, X. Zhao, G. Hu, W. Yue, X. Yuan, and J. Ren, *Physica E* **116**, 113729 (2020).
- [71] Z. Sun, H. Chu, Y. Li, S. Zhao, G. Li, and D. Li, *Materials and Design* **183**, 108129 (2019).
- [72] W. Kohn and L. J. Sham, *Phys. Rev.* **140**, A1133 (1965).
- [73] J. Taylor, H. Guo, and J. Wang, *Phys. Rev. B* **63**, 245407 (2001).
- [74] J. Taylor, H. Guo, and J. Wang, *Phys. Rev. B* **63**, 121104 (2001).
- [75] J. Bardeen, *Phys. Rev.* **71**, 717 (1947).
- [76] R. T. Tung, *Materials Science and Engineering: R: Reports* **35**, 1 (2001).
- [77] W. E. Spicer, P. W. Chye, P. R. Skeath, C. Y. Su, and I. Lindau, *Journal of Vacuum Science and Technology* **16**, 1422 (1979).
- [78] G. Grossi and G. P. Parravicini, *Solid state physics* (Academic Press: Cambridge, MA, USA, 2013).